Influence of temperature on the kinetics absorption of carbon dioxide in aqueous of enzyme catalysed MDEA solutions

Penders-van Elk, Nathalie J. M. C.; van Aken, Coen; Versteeg, Geert F.

Published in:
International Journal of Greenhouse Gas Control

DOI:
10.1016/j.ijggc.2016.02.021

International Journal of Greenhouse Gas Control 49 (2016) 64–72

Contents lists available at ScienceDirect

International Journal of Greenhouse Gas Control

journal homepage: www.elsevier.com/locate/ijggc

Influence of temperature on the kinetics of enzyme catalysed absorption of carbon dioxide in aqueous MDEA solutions

Nathalie J.M.C. Penders-van Elk[a,*], Coen van Aken[a,1], Geert F. Versteeg[b,**]

[a] Procede Gas Treating BV, P.O. Box 328, 7500 AH Enschede, The Netherlands
[b] University of Groningen, P.O. Box 72, 9700 AB Groningen, The Netherlands

ARTICLE INFO

Article history:
Received 2 October 2015
Accepted 15 February 2016
Available online 3 March 2016

Keywords:
Carbon dioxide capture
Carbonic anhydrase
MDEA
Kinetics
Temperature

ABSTRACT

In the present work the absorption of carbon dioxide in 1000 mol m^{-3} N-methyldiethanolamine (MDEA) solutions with and without enzyme has been studied in a stirred cell reactor in the temperature range 278–343 K and enzyme concentrations ranging from 0 to 1600 g m^{-3}. During this study a new type of carbonic anhydrase has been tested: the evolved tetrameric enzyme GS6-046. The kinetic data from the new enzyme has been compared to the kinetic data obtained with the thermostable CA mutant 5X and the new enzyme showed a faster kinetics towards the CO_2 hydration in combination with MDEA.

The experimental kinetic data from the evolved CA at the temperatures 278, 288 and 313 K resulted in a temperature dependent equation for the enzymatic rate constant $k^*_{H_2O}$. In the temperature range 278–313 K, this equation predicts $k^*_{H_2O}$ within an accuracy of 30%. However, at 343 K the measured $k^*_{H_2O}$ is significantly overestimated.

1. Introduction

Aqueous solutions of amines are frequently used for the removal of acid gases, such as carbon dioxide (CO_2) and hydrogen sulfide (H_2S), from a variety of gas streams. In particular, aqueous solutions of alkanolamines and blends of alkanolamines are widely applied in gas treating (Kohl and Nielsen, 1997). An example is the combination of N-methyldiethanolamine (MDEA) and monoethanolamine (MEA). Here the advantage of MEA, fast reacting primary alkanolamine and the lower regeneration temperature of MDEA are combined. However, this combination has a large disadvantage: the MEA is consumed during the reactive absorption. In order to maintain the positive effect, the use of a catalyst is preferable.

The enzyme carbonic anhydrase (CA), which is present in almost all living organisms, is a very efficient catalyst for the interconversion between CO_2 and HCO_3^- (Lindskog and Silverman, 2000). Due to its fast kinetics and the fact that it uses CO_2 as substrate, this enzyme has attracted the attention in CO_2 capture technologies (Cowan et al., 2003; Favre et al., 2009; Lu et al., 2011; Savile and Lalonde, 2011; Russo et al., 2013). However, the naturally derived enzyme is not stable in the conditions in CO_2 capture processes. By modification e.g. directed evolution (Alvizo et al., 2014), more stable enzymes have been created that can be used in the capture processes.

Penders-van Elk et al. (2013, 2015) derived a simplified mechanistic model for the enzymatic CO_2 absorption. However for amines, this model is only valid at 298 K. In the present work, the influence of the temperature on the enzymatic CO_2 absorption kinetics in 1000 mol m^{-3} MDEA solutions is investigated.

2. Theoretical background

2.1. Mass transfer

The absorption of gas A into a liquid is generally described by a.o. (Westerterp et al., 1984):

$$J_A = \frac{C_{A,G} - \frac{C_{A,L}}{m_A}}{\frac{1}{k_G} + \frac{1}{m_A k_L E_A}} \quad (1)$$

For a system consisting of a pure gas and assuming ideal gas behaviour and a freshly prepared and therefore lean liquid ($C_{A,L}$ = 0), Eq. (1) can be simplified to:

$$J_A = m_A k_L E_A \frac{P_A}{RT} \quad (2)$$

* Corresponding author.
** Principal corresponding author.
E-mail addresses: nathaliependers@procede.nl (N.J.M.C. Penders-van Elk), geertversteeg@procede.nl (G.F. Versteeg).
[1] Current address: Nedstack Fuel Cell Technology BV, P.O. Box 5167, 6802 ED Arnhem, The Netherlands.

http://dx.doi.org/10.1016/j.ijggc.2016.02.021
1750-5836/

Notation

A_{GL}	surface area of G/L interface (m^2)
C_A	concentration of A ($mol\,m^{-3}$)
D_A	diffusion coefficient of A ($m^2\,s^{-1}$)
E_A	enhancement factor of A (–)
J_A	flux of A ($mol\,m^{-2}\,s^{-1}$)
k_1	first order reaction rate constant (s^{-1})
k_2	second order reaction rate constant ($m^3\,mol^{-1}\,s^{-1}$)
k_L	liquid side mass transfer coefficient ($m\,s^{-1}$)
k_{OV}	overall reaction rate constant (s^{-1})
m_A	G/L distribution coefficient of A (–)
P	pressure (Pa)
R	gas constant ($8.314\,J\,mol^{-1}\,K^{-1}$)
R_A	reaction rate of A ($mol\,m^{-3}\,s^{-1}$)
T	temperature (K)
t	time (s)
V	volume (m^3)
ν_A	reaction order of A

Subscripts

0	initial
Am	amine
eq	equilibrium
G	gas phase
inf	infinite
L	liquid phase
vap	vapour

The chemical enhancement factor, E_A, is a function of the so-called Hatta number. When the absorption occurs in the first order regime and $Ha > 2$, the enhancement factor equals the Hatta number:

$$E_A = Ha = \frac{\sqrt{k_1 D_A}}{k_L} \tag{3}$$

For reactions different from the simple first-order reaction, the process can be considered in the pseudo-first order regime when next criterion is fulfilled:

$$2 < Ha \ll E_{inf} \tag{4}$$

where E_{inf} is the infinite enhancement factor. For irreversible reactions the infinite enhancement factor is defined as (van Swaaij and Versteeg, 1992):

$$E_{inf} = 1 + \frac{D_{Am}}{D_A}\frac{C_{Am}}{\nu_{Am}}\frac{RT}{m_A P_A} \tag{5}$$

2.2. Kinetics

When carbon dioxide is absorbed in an aqueous solution containing MDEA, following three reactions occur parallel and simultaneously:

- Reaction I – with MDEA (Versteeg and van Swaaij, 1988a; Littel et al., 1990; Benamor and Aroua, 2007)

$$CO_2 + R_3N + H_2O \rightleftharpoons HCO_3^- + R_3NH^+$$

- Reaction II – with hydroxide ion (Pinsent et al., 1956; Pohorecki and Moniuk, 1988)

$$CO_2 + OH^- \rightleftharpoons HCO_3^-$$

- Reaction III – with water (Pinsent et al., 1956; Kern, 1960)

$$CO_2 + 2H_2O \rightleftharpoons HCO_3^- + H_3O^+$$

The overall forward reaction rate constant, k_{OV}, is determined by the contributions of each of these three reactions, whose kinetic rate expression is usually given as follows:

- Reaction I:

$$R_{CO_2,I} = k_{Am} C_{Am} C_{CO_2} = k'_{Am} C_{CO_2} \tag{6}$$

- Reaction II:

$$R_{CO_2,II} = k_{OH} C_{OH^-} C_{CO_2} = k'_{OH} C_{CO_2} \tag{7}$$

- Reaction III:

$$R_{CO_2,III} = k_{H_2O} C_{CO_2} = k'_{H_2O} C_{CO_2} \tag{8}$$

In the absence of any mass transfer limitations, the overall forward pseudo-first order reaction rate constant is defined as the sum of these rates divided by the concentration of carbon dioxide.

$$k_{OV} = k'_{Am} + k'_{OH} + k'_{H_2O} \tag{9}$$

In the presence of the enzyme carbonic anhydrase the reaction mechanism is extended with the following "wheel of reactions" (Lindskog and Silverman, 2000; Larachi, 2010):

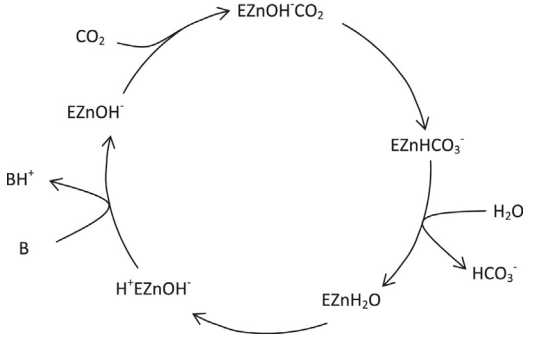

The base used during enzyme regeneration can either be the carbonate ion, the hydroxide ion, the alkanolamine or even the during the reaction formed bicarbonate ion (Larachi, 2010). In the latter case, carbon dioxide and water are released as protonated base.

In the presence of the enzyme carbonic anhydrase, reaction III is the most important reaction during absorption of carbon dioxide into aqueous MDEA solutions (Penders-van Elk et al., 2012). It is common to define reaction III, CO_2 hydration, as a pseudo-first order reaction, thus zeroth order in water, assuming that the water concentration does not change (Kern, 1960). However, this reaction is actually a second order reaction (Wang et al., 2010). This was confirmed by Penders-van Elk et al. (2012) in the determination of the enzyme kinetics over a wide range of water concentrations. For the enzymatic CO_2 hydration the water concentration is no longer a constant, so it is no longer valid to assume pseudo-first order kinetics for reaction III. Therefore, next equation should be used for the kinetic rate expression:

$$R_{CO_2,III} = k_{H_2O} C_{H_2O} C_{CO_2} = k'_{H_2O} C_{CO_2} \tag{10}$$

And the forward reaction rate constant for the enzyme catalysed reaction is calculated as:

$$k^*_{H_2O} = \frac{k_{OV,\,with\,enzyme} - k_{OV,\,without\,enzyme}}{C_{H_2O}} \tag{11}$$

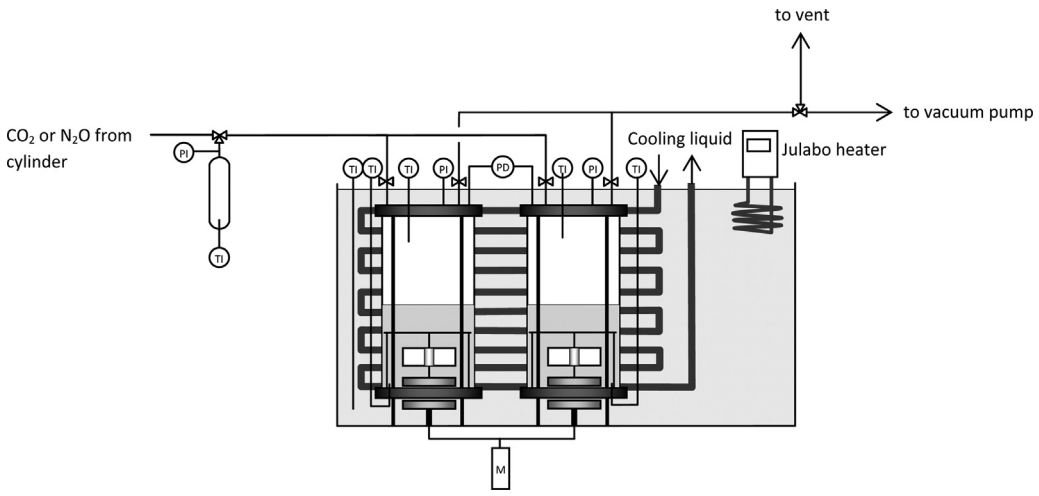

Fig. 1. Schematic drawing of the experimental set-up.

Eq. (11) is only valid if the experiments are in the pseudo-first order regime for all reactions involved.

The following empirical equation describes the relation between $k^*_{H_2O}$ and the enzyme concentration (Penders-van Elk et al., 2013):

$$k^*_{H_2O} = \frac{k^*_3 C_{Enz}}{1 + k^*_4 C_{Enz}} \tag{12}$$

3. Materials and Methods

3.1. Materials

3.1.1. Experimental setup

All absorption experiments have been performed in a thermostatted stirred cell type reactor operated with a smooth and horizontal gas–liquid interface. The reactor was connected to two gas supply vessels filled with carbon dioxide or nitrous oxide from gas cylinders. Both the reactor and gas supply vessels were equipped with digital pressure transducers and PT-100 thermocouples. The measured signals were recorded in a computer. The pressure transducers connected to the stirred cell reactors were Ashcroft pressure transducers (range 0–2.5 bara) and the gas supply vessel was equipped with an Ashcroft pressure transducer (range 0–10 bara). A schematic drawing of the experimental set-up is shown in Fig. 1.

3.1.2. Chemicals

The N-methyldiethanolamine used for the preparation of the aqueous solutions had a purity of >99% and it was used as supplied by Aldrich. The enzyme used an evolved form of a tetrameric (4 unit) enzyme developed by Codexis named GS6-046. All solutions were prepared with deminaralised water. The carbon dioxide (>99.9%) and nitrous oxide (99.5%) were obtained from Air Liquide.

3.2. Method

The measurements of the N_2O or CO_2 absorption into aqueous MDEA in presence or absence of the enzyme were performed in batch mode with respect to both liquid and gas phase. In a typical experiment approximately 500 ml solution with the desired composition was added to the reactor. The system was evacuated to remove inerts from the solution. Then it was allowed to equilibrate at the desired temperature and the vapour pressure (P_{vap}) was recorded. Also the pressure and temperature in the gas supply vessel were recorded. Then a predetermined amount of N_2O or CO_2 was fed to the reactor from the gas bomb to obtain a desired pressure in the reactor (P_0) and then the stirrer (approx. 100 rpm) was turned on at such a speed that the flat gas–liquid interface was maintained. The decrease in total pressure was recorded. By subtracting the solution's vapour pressure from the total pressure, the partial pressure for N_2O or CO_2 is obtained. At the end of the experiment the final pressure in the reactor (P_{eq}) together with the pressure and temperature in the gas supply vessel were recorded.

The experiments have been performed with aqueous MDEA solutions at 278, 288, 298, 313 and 343 K respectively. The MDEA concentration for all experiments was 1000 mol m^{-3}, as previous study (Penders-van Elk et al., 2012) showed that the concentration of MDEA has no effect on the reaction rate constants. The enzyme concentration has been varied between 0 and 1.6 kg m^{-3}.

3.2.1. Overall forward kinetic rate constant

For a pseudo-first order reaction, a carbon dioxide balance over the gas phase in combination with Eqs. (2) and (3) yields:

$$\frac{\mathrm{d} \ln P_{CO_2}}{\mathrm{d}t} = -\sqrt{k_{OV} D_{CO_2}} \frac{A_{GL} m_{CO_2}}{V_G} \tag{13}$$

Typically, a plot of the natural logarithm of the carbon dioxide partial pressure versus time will yield a straight line with a constant slope, from which the overall kinetic rate constant, k_{OV} can be determined, once the required physico-chemical constants are known.

3.2.2. Distribution coefficient

If possible, literature correlations are used to calculate the distribution coefficient of nitrous oxide for 1000 mol m^{-3} MDEA solution (Al-Ghawash et al., 1989; Wang et al., 1992). However, at 278 and 343 K the distribution coefficient had to be determined experimentally. Therefore, N_2O absorption experiments were performed at these temperatures. The distribution coefficient was calculated as:

$$m = \left(\frac{C_L}{C_G}\right)_{eq} = \frac{RT}{He} = \frac{P_0 - P_{eq}}{P_{eq} - P_{vap}} \cdot \frac{V_G}{V_L} \tag{14}$$

With the CO_2–N_2O analogy the distribution coefficients for carbon dioxide were obtained.

$$m_{CO_2,MDEA} = m_{CO_2,water} \frac{m_{N_2O,MDEA}}{m_{N_2O,water}} \tag{15}$$

Table 1
Distribution coefficient of nitrous oxide for the experimental conditions.

Temperature (K)	$m_{N_2O,MDEA}$ (−)	Ref.
278	1.00	This study
288	0.77	Al-Ghawash et al. (1989)
298	0.586	Wang et al. (1992)
313	0.43	Wang et al. (1992)
343	0.225	This study

The ratio of the solubility of CO_2 in water over N_2O in water was calculated with the correlation developed by Versteeg and van Swaaij (1988b):

$$\frac{m_{CO_2,water}}{m_{N_2O,water}} = 3.04 \cdot \exp\left(-\frac{240}{T}\right) \quad (16)$$

The distribution coefficients as used in the evaluation of the experiments are listed in Table 1.

3.2.3. Diffusion coefficient

The diffusion coefficient of carbon dioxide is estimated from the solution's viscosity using the Stokes–Einstein relationship (Versteeg and van Swaaij, 1988b):

$$D_{CO_2,\ MDEA} = D_{CO_2,\ water}\left(\frac{\eta_{water}}{\eta_{MDEA}}\right)^{0.8} \quad (17)$$

The diffusion coefficient of carbon dioxide in water was calculated using the correlation given by Jamal (2002). The viscosity of water was taken from Perry's Chemical Engineers' Handbook (Perry et al., 1997). The viscosity of the MDEA solutions was calculated using the correlations given by Al-Ghawash et al. (1989).

4. Results

4.1. 278 K

CO_2 absorption experiments have been performed with 1000 mol m^{-3} MDEA solutions at 278 K with CA mutant GS6-046. The enzyme concentration has been varied from 0 to 1.6 kg m^{-3}. The results of these experiments presented in Fig. 2.

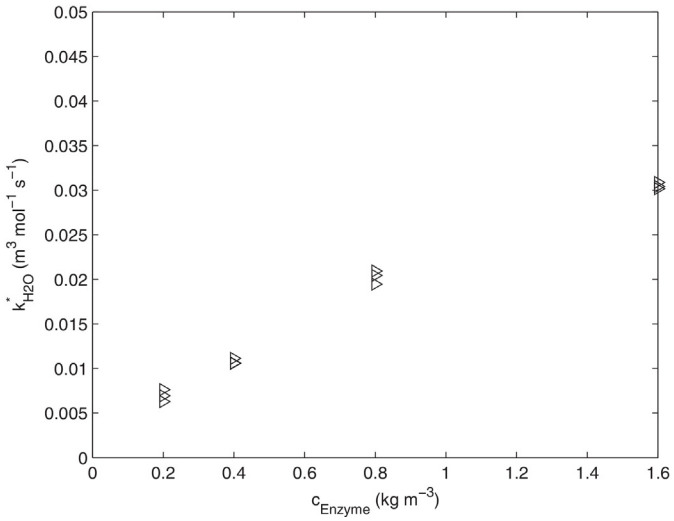

Fig. 2. The results of experiments performed with the evolved tetrameric enzyme GS6-046 at 278 K.

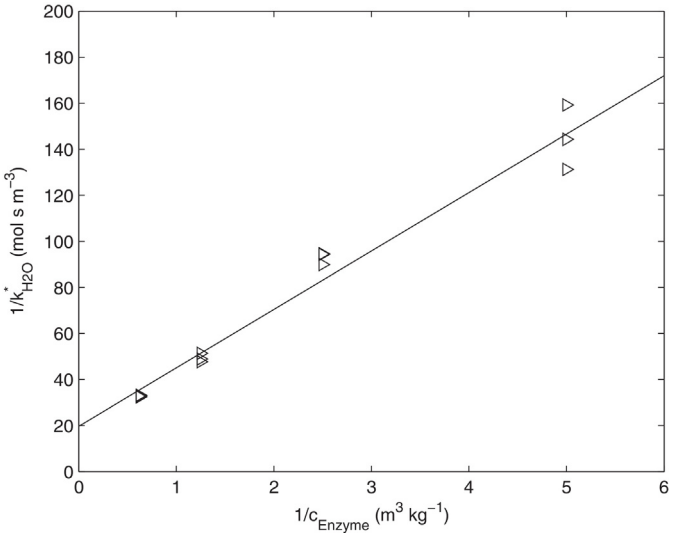

Fig. 3. The linearised results of experiments performed at 278 K. The line represents the trend line for the results with the enzyme GS6-046.

By taking the double reciprocal of Eq. (12), the empirical correlation for $k^*_{H_2O}$ is linearised, resulting in:

$$\frac{1}{k^*_{H_2O}} = \frac{1}{k^*_3}\frac{1}{C_{Enz}} + \frac{k^*_4}{k^*_3} \quad (18)$$

From the linearised results for $k^*_{H_2O}$ presented in Fig. 3 k^*_3 and k^*_4 have been determined to be 0.039 m^6 mol^{-1} kg^{-1} s^{-1} and 0.78 m^3 kg^{-1} respectively.

4.2. 288 K

At 288 K, CO_2 absorption experiments were performed with only the enzyme GS6-046 in the concentration range 0–1.6 kg m^{-3}. The results of these experiments are presented in Fig. 4.

From the linearised results for k^*_{H2O} presented in Fig. 5 k^*_3 and k^*_4 are determined to be 0.045 m^6 mol^{-1} kg^{-1} s^{-1} and 0.67 m^3 kg^{-1} respectively.

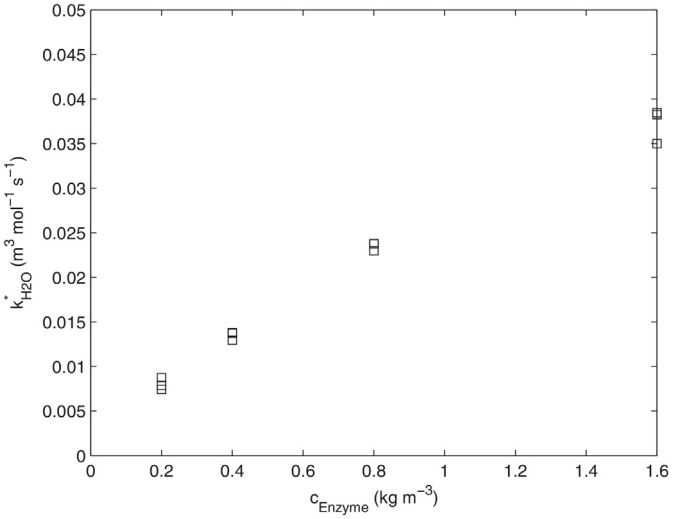

Fig. 4. The results of experiments with the evolved tetrameric enzyme GS6-046 performed at 288 K.

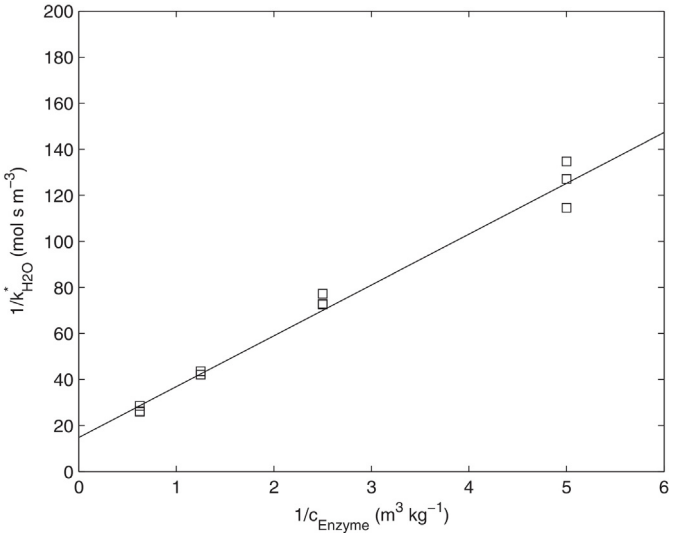

Fig. 5. The linearised results of experiments performed at 288 K. The line represents the trend line.

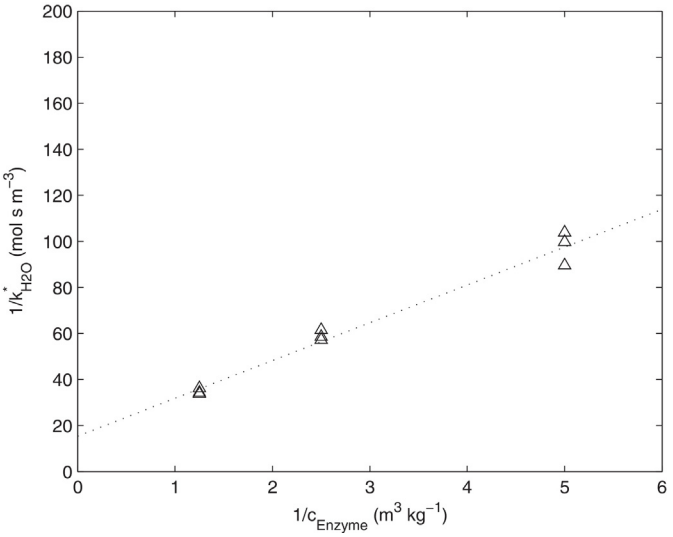

Fig. 7. The linearised results of experiments performed at 298 K. The dotted line represents the trend line.

4.3. 298 K

At 298 K, only up to an enzyme concentration of 0.8 kg m^{-3} experiments were performed. The results of these experiments are presented in Fig. 6.

From the linearised results for k^*_{H2O} presented in Fig. 7 k^*_3 and k^*_4 are determined to be 0.061 m^6 mol^{-1} kg^{-1} s^{-1} and 0.94 m^3 kg^{-1} respectively. Because of the small enzyme concentration range these determined k^*_3 and k^*_4 will not be used in further analysis due to the relative large uncertainty in the values.

4.4. 313 K

At 313 K, CO_2 absorption experiments were performed with CA mutant GS6-046 in the enzyme concentration range 0–1.6 kg m^{-3}. The results of these experiments are presented in Fig. 8.

From the linearised results for k^*_{H2O} presented in Fig. 9 k^*_3 and k^*_4 are determined to be 0.058 m^6 mol^{-1} kg^{-1} s^{-1} and 0.77 m^3 kg^{-1} respectively.

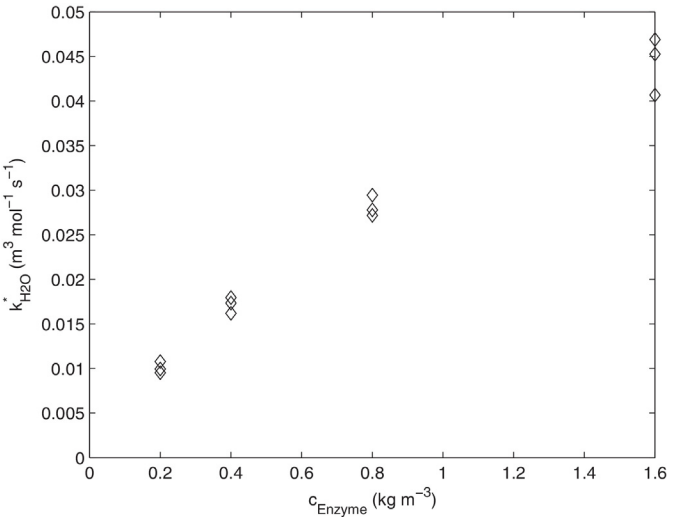

Fig. 8. The results of experiments with the evolved tetrameric enzyme GS6-046 performed at 313 K.

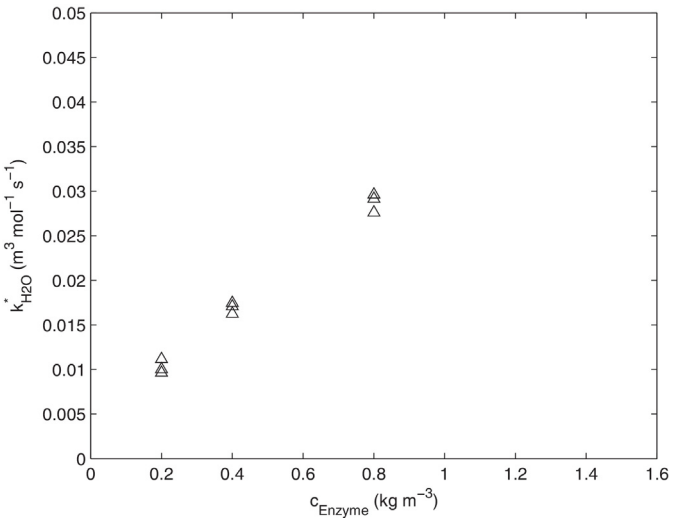

Fig. 6. The results of experiments with the evolved tetrameric enzyme GS6-046 performed at 298 K.

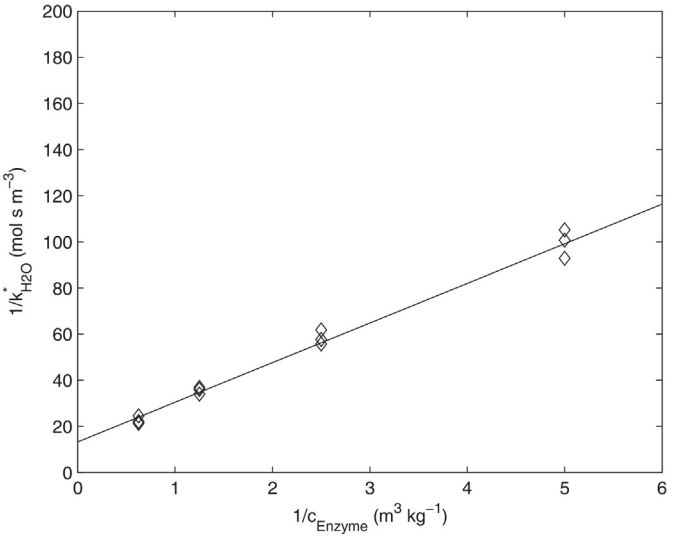

Fig. 9. The linearised results of experiments performed at 313 K. The line represents the trend line.

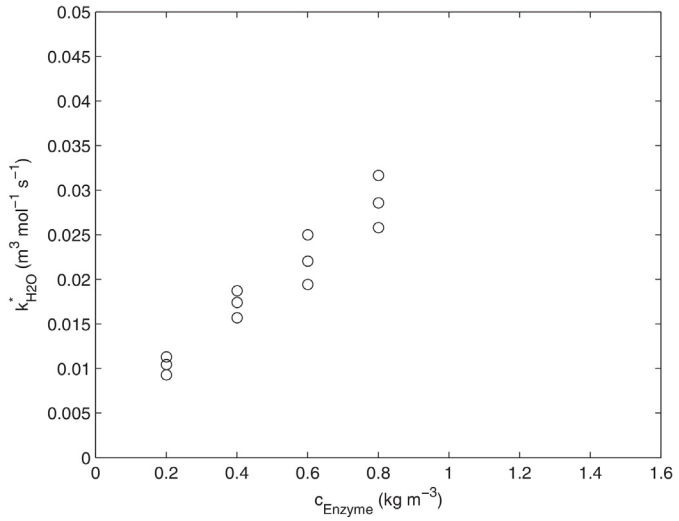

Fig. 10. The results of experiments with the evolved tetrameric enzyme GS6-046 performed at 343 K.

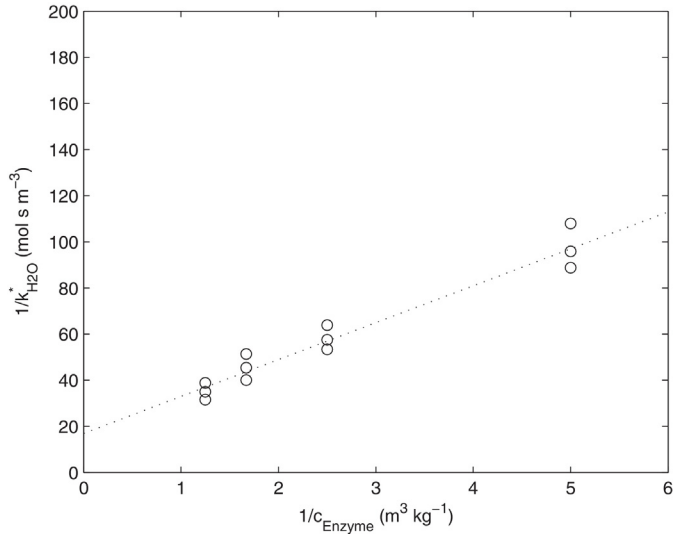

Fig. 11. The linearised results of experiments performed at 343 K. The line represents the trend line.

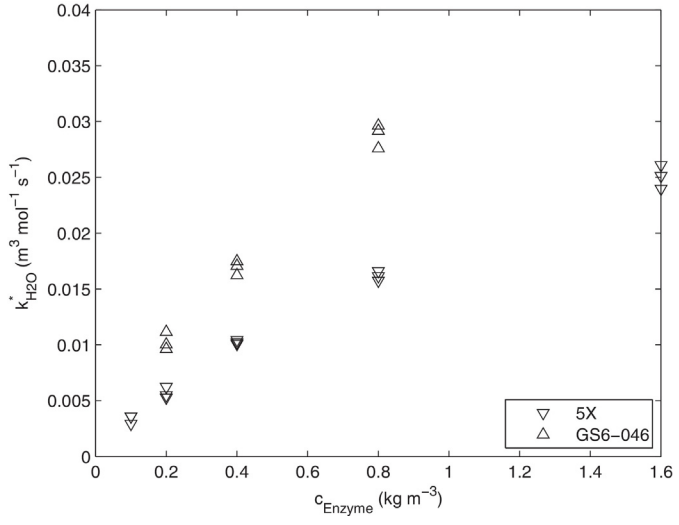

Fig. 12. The rate constant for the enzyme catalysed CO_2 hydration for CA mutant 5X and for the evolved tetrameric enzyme GS6-046 at 298 K.

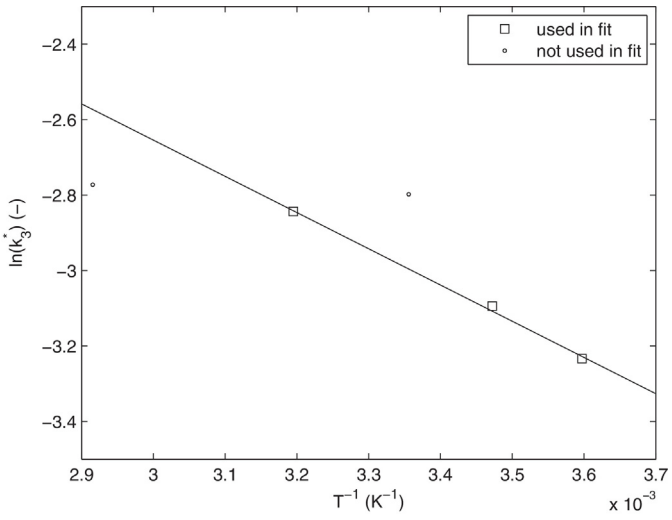

Fig. 13. Arrhenius plot for the kinetic constant k^*_3.

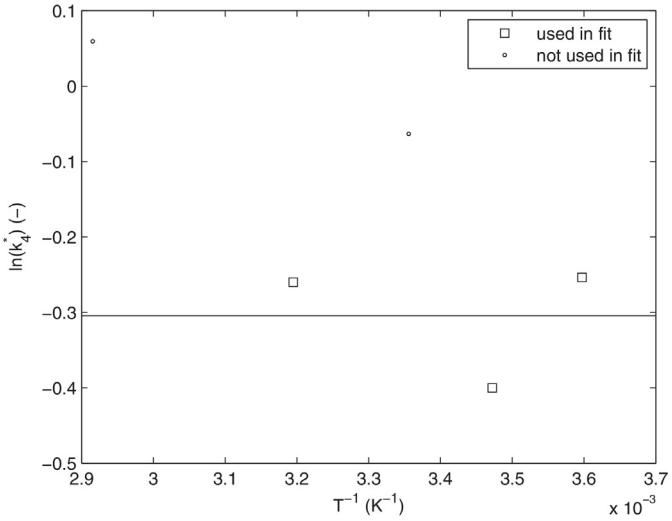

Fig. 14. Arrhenius plot for the kinetic constant k^*_4.

4.5. 343 K

At 343 K, only up to an enzyme concentration of 0.8 kg m^{-3} experiments were performed. The results of these experiments are presented in Fig. 10.

From the linearised results for $k^*_{H_2O}$ presented in Fig. 11 k^*_3 and k^*_4 are determined to be 0.063 m^6 mol^{-1} kg^{-1} s^{-1} and 1.1 m^3 kg^{-1} respectively. Because of the small enzyme concentration range these k^*_3 and k^*_4 they will not be used in further analysis due to the relative large uncertainty in the values.

5. Discussion

5.1. CA mutant 5X vs. evolved tetrameric CA GS6-046

In order to see if previous experimental data obtained with the CA mutant 5X (Penders-van Elk et al., 2012, 2013) can be used to expand the limited range of this studies experiments at 298 K, the experimental results have to be compared with respect to $k^*_{H_2O}$. This comparison shows that the CA mutant 5X has a slower CO_2 hydration kinetics than the evolved enzyme GS6-046 used in this study (see Fig. 12). Therefore the data from previous studies

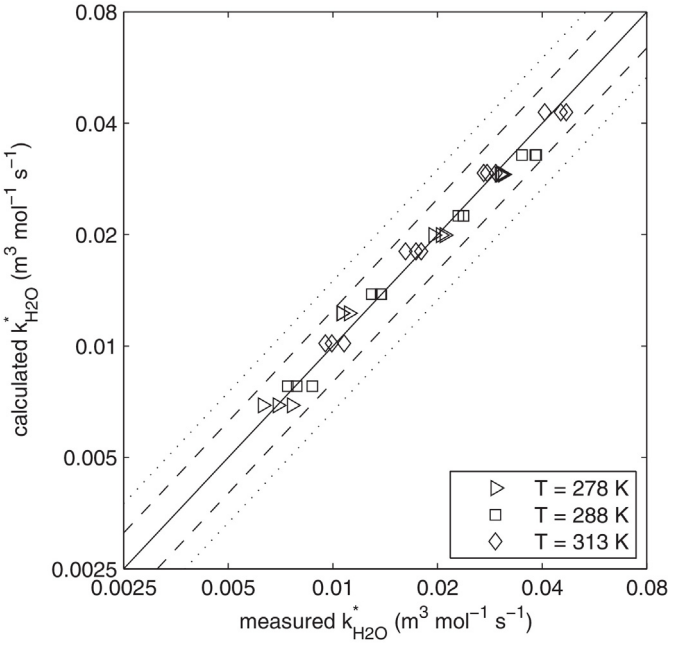

Fig. 15. Parity plot of the enzymatic kinetic constant for the enzyme GS6-046 at the temperatures used in the fit.

cannot be used in this analysis of the influence of temperature on the enzyme catalysed CO_2 hydration kinetics.

5.2. Influence of temperature

Now the results for the kinetic constants of k_3^* and k_4^* for the evolved tetrameric enzyme GS6-046 are known, their dependency on the temperature can be determined. In this determination only data obtained at 278, 288 and 313 K has been used. Figs. 13 and14 show the Arrhenius plots for k_3^* and k_4^* together with the trend lines, respectively. The trend lines can be described with following two equations:

$$k_3^* = 1.3 \exp\left(\frac{-960}{T}\right) \tag{19}$$

$$k_4^* = 0.74 \tag{20}$$

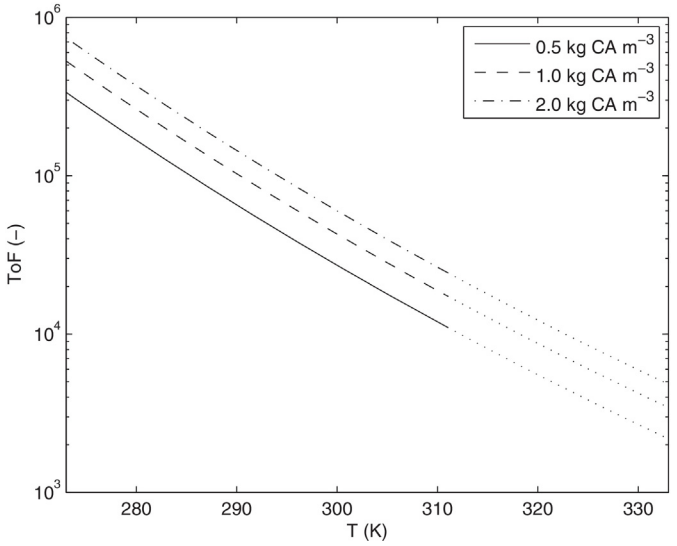

Fig. 17. The turnover factor as function of the temperature calculated at three enzyme concentrations.

Substituting above equations in Eq. (12) gives:

$$k^*_{H_2O} = \frac{1.3 \exp\left(\frac{-960}{T}\right) C_{Enz}}{1 + 0.74 \cdot C_{Enz}} \tag{21}$$

At the temperatures used in the fit, this equation predicts the measured $k^*_{H_2O}$ for the enzyme GS6-046 within an accuracy of 20% (see Fig. 15), with an average deviation of 6%.

According to Eq. (19) k_3^* should be 0.050 m^6 mol^{-1} kg^{-1} s^{-1} at 298 K and 0.076 m^6 mol^{-1} kg^{-1} s^{-1} at 343 K, while according to Eq. (20) k_4^* is 074 m^3 kg^{-1} for both temperatures. Substitution of these values for the kinetic constants into Eq. (12) shows that the measured $k^*_{H_2O}$ at 298 K is on average 15% underestimated while at 343 K it is on average 36% overestimated (see Fig. 16). An explanation for this last observation might be that some kind of denaturation occurred at 343 K. Due to the limited available amount of the enzyme GS6-046 no experiments were performed to validate this statement.

6. Towards application

As mentioned in the theoretical background, the enzyme catalyses reaction III, the CO_2 hydration. Based on the data presented

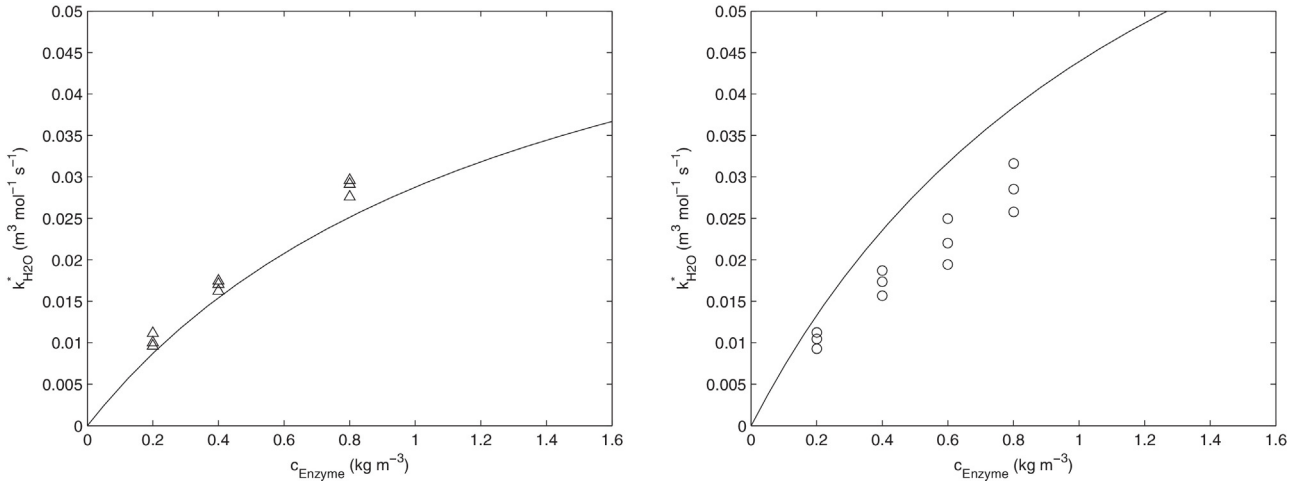

Fig. 16. The measured and predicted $k^*_{H_2O}$ at the temperatures: (left) at 298 K and (right) at 343 K.

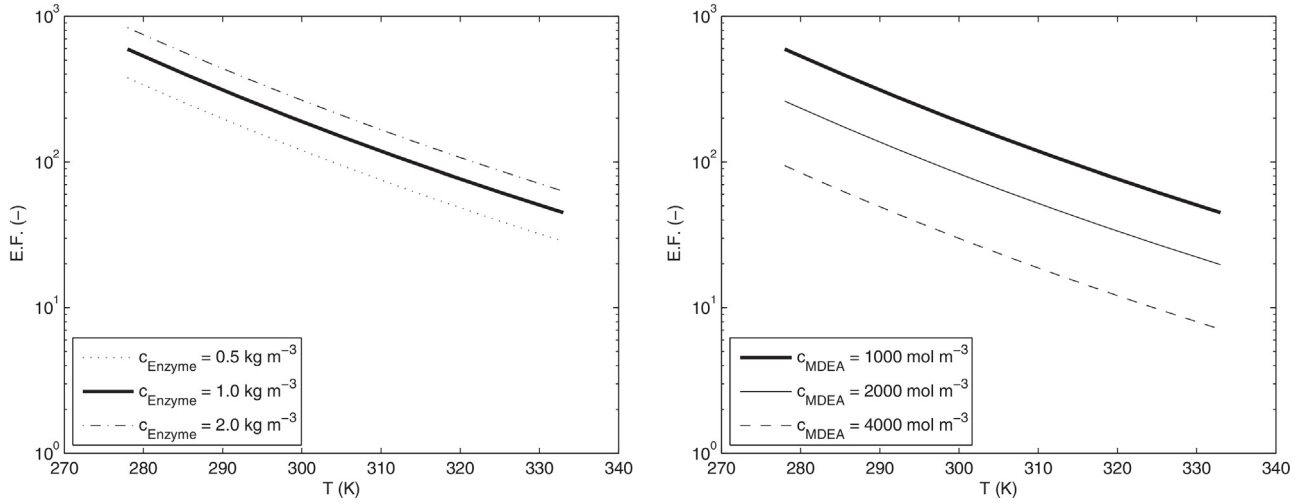

Fig. 18. The enhancement factor as function of the temperature calculated for solutions with (left) 1000 mol m^{-3} MDEA in combination with three enzyme concentrations and (right) three MDEA concentrations in combination with an enzyme concentration of 1 kg m^{-3}.

by amongst others Faurholt (1924), Stadie and O'Brien (1933), Brinkman et al. (1934), Kiese and Hastings (1940), Mills and Urey (1940), Roughton (1941), Pinsent et al. (1956), Welch et al. (1969), Johnson (1982), Soli and Byrne (2002), Wang et al. (2010), the following equation has been derived for the temperature dependency of the uncatalysed reaction rate constant k_{H_2O}:

$$k_{H_2O}(T) = 1.94 \cdot 10^6 \cdot \exp\left(\frac{-8590}{T}\right) \quad (22)$$

This equation is only valid in the temperature range 273–316 K.

To demonstrate the influence of temperature on the efficiency of the enzyme during the CO_2 hydration, the turnover factor and the enhancement factor are introduced:

$$ToF = \frac{R_{CO_2\ \text{hydration, with enzyme}}}{R_{CO_2\ \text{hydration, without enzyme}}} = \frac{k^*_{H_2O}}{k_{H_2O}} \quad (23)$$

$$EF = \frac{R_{CO_2,\ \text{with enzyme}}}{R_{CO_2,\ \text{without enzyme}}} = 1 + \frac{k^*_{H_2O} C_{H_2O}}{k_{MDEA} C_{MDEA}} \quad (24)$$

The results of the calculated turnover factor at various enzyme concentrations and temperatures, presented in Fig. 17, show that the turnover factor increases with increasing enzyme concentration, and decreases with increasing temperature.

The results of the calculated enhancement factor at various enzyme and MDEA concentrations and temperatures, presented in Fig. 18, show that the enhancement factor decreases with increasing temperature. Due to the relative fast kinetics of the more concentrated MDEA solution and due to the fact that $k^*_{H_2O}$ is independent of the MDEA concentration, the enhancement factor decreases with increasing MDEA concentration even though the enzyme concentration is increased. Furthermore, Fig. 18 shows that at temperatures over 320 K the influence of the temperature on the enhancement factor is no longer significant, meaning that the rate of the uncatalysed CO_2 absorption in MDEA is in the same order of magnitude as the rate of the enzyme catalysed CO_2 absorption.

7. Conclusions

The kinetics of CO_2 with a 1000 mol m^{-3} MDEA solution in presence of the evolved tetrameric enzyme GS6-046, has been studied in the temperature range 278–343 K. The relation derived from the kinetic data of the enzyme GS6-046 at the temperatures 278, 288 and 313 K described the all measurements performed in the temperature range 278–313 K within 30% accuracy. However, at 343 K, the measured kinetics are on average 36% overestimated. The most likely explanation might be partial denaturation of the enzyme GS6-046 occurred at 343 K. However, due to the limited available amount of the enzyme this statement has not been verified.

When applying enzyme in the absorption process, the absorption is most enhanced at low temperatures. Because the enzyme kinetics is less temperature dependent than the kinetics of the other reactions, the enhancement obtained by applying the enzyme decreases with increasing temperatures. Over the temperature range 278–333 K the enhancement factor decreased from 600 to 45 for a 1000 mol m^{-3} MDEA solution with 1 kg m^{-3} enzyme. Thus, there is no need for a more temperature stable enzyme than the enzyme GS6-046 used in this research. To increase the lifetime of the enzyme, it is more important to look for techniques to separate the enzyme from the solvent before it enters the desorber for regeneration.

Acknowledgement

Codexis, Inc., Redwood City, CA, U.S.A. is acknowledged for the supply of the enzyme GS6-046.

References

Al-Ghawash, H., Hagewiesche, D., Ruiz-Ibanez, G., Sandall, O., 1989. Physocochemical properties important for carbon dioxide absorption in aqueous methyldiethanolamine. J. Chem. Eng. Data 34, 385–391.

Alvizo, O., Nguyen, L., Savile, C., Bresson, J., Lakhapatri, S., Solis, A., Fox, R., Broering, J., Benoit, M.R., abd Zimmerman, S., Novick, S., Liang, J., Lalonde, J., 2014. Directed evolution if an ultrastable carbonic anhydrase for highly efficient carbon capture from flue gas. PNAS 111, 16436–16441.

Benamor, A., Aroua, M., 2007. An experimental investigation on the rate of CO_2 absorption into aqueous methyldiethanolamine solutions. Kor. J. Chem. Eng. 24, 16–23.

Brinkman, R., Margaria, R., Roughton, F., 1934. The kinetics of the carbon dioxide-carbonic acid reaction. Philos. Trans. R. Soc. London. Ser. A 232, 65–97.

Cowan, R., Ge, J.J., Qin, Y.J., McGregor, M., Trachtenberg, M., 2003. CO_2 capture by means of an enzyme-based reactor. Ann. New York Acad. Sci. 984, 453–469.

Faurholt, C., 1924. Études sur les solutions aqueuses d'anhydride carbonique et d'acide carbonique. J. Chim. Phys. 21, 400–455.

Favre, N., Lorraine, C., Pierre, A., 2009. Biocatalytic capture of CO_2 with carbonic anhydrase and its transformation to solid carbonate. J. Mol. Catal. B: Enzym. 60, 163–170.

Jamal, A., 2002. Absorption and desorption of CO_2 and CO in alkanolamine systems. The University of British Colombia, Canada (Ph.D. thesis).

Johnson, K., 1982. Carbon dioxide hydration and dehydration kinetics in seawater. Limnol. Oceanogr. 27, 849–855.

Kern, D., 1960. The hydration of carbon dioxide. J. Chem. Educ. 37, 14–23.

Kiese, M., Hastings, A., 1940. The catalytic hydration of carbon dioxide. J. Biol. Chem. 132, 267–280.

Kohl, A., Nielsen, R., 1997. Gas Purification, 5th ed. Elsevier.
Larachi, F., 2010. Kinetic model for the reversible hydration of carbon dioxide catalyzed by human carbonic anhydrase II. Indus. Eng. Chem. Res. 49, 9095–9104.
Lindskog, S., Silverman, D., 2000. The catalytic mechanism of mammalian carbonic anhydrases. In: Chegwidden, W., Carter, N., Edwards, Y. (Eds.), The Carbonic Anhydrases – New Horizons. Birkhäuser Verlag, Basel, Switzerland, pp. 175–195.
Littel, R., van Swaaij, W., Versteeg, G., 1990. Kinetics of carbon dioxide with tertiary amines in aqueous solution. AIChE J. 36, 1633–1640.
Lu, Y.X., Zhang, Y., Khodayari, Z., Djukadi, A.T., 2011. Development of a carbonate absorption-based process for post-combustion CO_2 capture: the role of biocatalyst to promote CO_2 absorption rate. Energy Procedia 4, 1286–1293.
Mills, G., Urey, H., 1940. The kinetics of isotopic exchange between carbon dioxide, bicarbonate ion, carbonate ion and water. J. Am. Chem. Soc. 62, 1019–1026.
Penders-van Elk, N., Derks, P., Fradette, S., Versteeg, G., 2012. Kinetics of absorption of carbon dioxide in aqueous MDEA solutions with carbonic anhydrase at 298 K. Int. J. Greenh. Gas Control 9, 385–392.
Penders-van Elk, N., Fradette, S., Versteeg, G., 2015. Effect of pKa on the kinetics of carbon dioxide absorption in aqueous alkanolamine solutions containing carbonic anhydrase at 298 K. Chem. Eng. J. 259, 682–691.
Penders-van Elk, N., Hamborg, E., Huttenhuis, P., Fradette, S., Carley, J., Versteeg, G., 2013. Kinetics of absorption of carbon dioxide in aqueous amine and carbonate solutions with carbonic anhydrase. Int. J. Greenh. Gas Control 12, 259–268.
Perry, R., Green, D., Maloney, J., 1997. Perry's Chemical Engineers' Handbook, 7th ed. McGraw-Hill.
Pinsent, B., Pearson, L., Roughton, F., 1956. The kinetics of combination of carbon dioxide with hydroxide ions. Trans. Faraday Soc. 52, 1512–1520.
Pohorecki, R., Moniuk, W., 1988. Kinetics of the reaction between carbon dioxide and hydroxyl ions in aqueous electrolyte solutions. Chem. Eng. Sci. 43, 1677–1684.
Roughton, F., 1941. The kinetics and rapid thermochemistry of carbonic acid. J. Am. Chem. Soc. 63, 2930–2934.
Russo, M., Olivieri, G., Marzocchella, A., Salatino, P., Caramuscio, P., Cavaleiro, C., 2013. Post-combustion carbon capture mediated by carbonic anhydrase. Sep. Purif. Technol. 107, 331–339.
Savile, C., Lalonde, J., 2011. Biotechnology for the acceleration of carbon dioxide capture and sequestration. Curr. Opin. Biotechnol. 22, 818–823.
Soli, A., Byrne, R., 2002. CO_2 system hydration and dehydration kinetics and the equilibrium CO_2/H_2CO_3 ratio in aqueous NaCl solution. Marine Chem. 78, 65–73.
Stadie, W., O'Brien, H., 1933. The catalysis of the hydration of carbon dioxide and dehydration of carbonic acid by an enzyme isolated from red blood cells. J. Biol. Chem. 103, 521–529.
van Swaaij, W., Versteeg, G., 1992. Mass transfer accompanied with complex reversible chemical reactions in gas-liquid systems: an overview. Chem. Eng. Sci. 47, 3181–3195.
Versteeg, G., van Swaaij, W., 1988a. On the kinetics between CO_2 and alkanolamines both in aqueous and non-aqueous solutions – II tertiary amines. Chem. Eng. Sci. 43, 587–591.
Versteeg, G., van Swaaij, W., 1988b. Solubility and diffusivity of acid gases (CO_2, N_2O) in aqueous alkanolamine solutions. J. Chem. Eng. Data 33, 29–34.
Wang, X., Conway, W., Burns, R., McCann, N., Maeder, M., 2010. Comprehensive study of the hydration and dehydration reactions of carbon dioxide in aqueous solution. J. Phys. Chem. A 114, 1734–1740.
Wang, Y., Xu, S., Otto, F., Mather, A., 1992. Solubility of N_2O in alkanolamines and in mixed solvents. Chem. Eng. J. 48, 31–40.
Welch, M., Lifton, J., Seck, J., 1969. Tracer studies with radioactive oxygen-15. Exchange between carbon dioxide and water. J. Phys. Chem. 73, 3351–3356.
Westerterp, K., van Swaaij, W., Beenackers, A., 1984. Chemical Reactor Design and Operation. John Wiley & Sons Ltd.